Supporting Information

All-Printed Flexible Heaters based on Dendritic Ag Inks for Heatable Packaging Applications

Linlong He[a, b], Xiting Xie[a, b], Shuiling Zhang[a], Shang Liu[a], Zengxinyue He[a], Jing Liang[b], Heping Zhu[a], Wei Wu[b]**

[a] School of Packaging Design and Art and School of Packaging and Materials Engineering, Hunan University of Technology, Zhuzhou 412007, P. R. China

[b] Laboratory of Printable Functional Materials and Printed Electronics, School of Physics and Technology, Wuhan University, Wuhan 430072, P. R. China

I. Experiment Section

Materials. Silver nitrate ($AgNO_3$, AR), anhydrous ethanol (C_2H_5OH, AR), ethylene glycol (EG, $C_2H_6O_2$, AR), copper chloride dihydrate ($CuCl_2 \cdot 2H_2O$), polyvinyl alcohol (PVA), Sinopharm Chemical Reagent Co., Ltd. polyvinyl pyrrolidone (PVP) are purchased from Sigma-Aldrich. The 822-nylon transparent paste (acrylate polymer emulsion: 30-40 wt%) is purchased from Jiangshan Bocai Chemical Co., Ltd. Hydroxylamine (H_3NO, 50 wt% in H_2O) is purchased from Aladdin reagent Co., Ltd.

Synthesis of Ag NWs. Ag NWs are synthesized by polyol reduction method. First, 0.01514 g of copper chloride dihydrate ($CuCl_2 \cdot 2H_2O$) is evenly dispersed in 40 mL of ethylene glycol (EG) to obtain $CuCl_2$/EG solution. Then, 1.665 g of PVP is evenly dispersed in 95 mL of EG by magnetic stirring. After stirring for 1.5 h, 5 mL of $CuCl_2$/EG solution is added into this solution (Solution A). Then, 1.79 g of $AgNO_3$ is added into 100 mL of EG and stirred to obtain solution B. Then, solution A is added

dropwise to solution B, and after sufficient stirring, it was poured into a polytetrafluoroethylene-lined autoclave and reacted at 160 °C for 3 hours. Finally, after the reaction solution was cooled to room temperature, the reaction product was centrifuged and washed three times with anhydrous ethanol and deionized water in turn, and pure Ag NWs are collected.

Formulation of Ag NWs-based conductive ink. 2 g of PVA is dissolved in 18 mL of deionized water under heating conditions at 90 °C to prepare a PVA aqueous solution. Then 1 g of Ag NWs is mixed with 2 g of PVA aqueous solution to obtain an Ag NWs-based conductive ink with a mass fraction of 35 wt%.

Formulation of Ag Flakes-based conductive ink. 2.4 g of Ag flakes is mixed with 3.0857 g of nylon transparent paste and 1.3714 g of solvent (composed of ethylene glycol, ethanol and deionized water in a ratio of 2:2:1) to obtain an Ag flakes-based conductive ink with a mass fraction of 35 wt%.

Synthesis of Ag FDs. The synthesis of Ag FDs was achieved by a simple redox reaction at room temperature. 1.02 g of Ag NO_3 and 1.5 mL of hydroxylamine are dispersed in 75 mL of deionized water to obtain solution A and solution B, respectively. Solution A and solution B are added dropwise to a three-necked flask at a magnetic stirring speed of 600 rpm for reaction, and the precipitate after the reaction was collected. After that, the precipitate is centrifuged and washed with deionized water, and the centrifugation process was repeated 3 times to collect pure Ag FDs.

Formulation of Ag FDs-based conductive ink. 2.4 g of Ag FDs is mixed with 3.0857 g of nylon transparent slurry and 1.3714 g of solvent (composed of ethylene glycol,

ethanol and deionized water in a ratio of 2:2:1) to obtain Ag FDs-based conductive ink with a mass fraction of 35 wt%.

Characterization. The viscoelasticity of the ink is tested using a rotational rheometer (Anton Paar MCR102e). The surface and cross-sectional morphology of the screen-printed electrode samples are characterized using a field-emission scanning electron microscope (TESCAN MIRA LMS) at a working voltage of 5 kV. The silver nanomaterials with different morphologies (Ag NWs, Ag Flakes, Ag FDs) are synthesized, and the as-formulated inks are deposited on substrates using a 150-mesh screen printing plate. The thermal properties of the MWE were performed with an IR camera (FLIR C3) with a matching analysis tool (FLIR Tools+, FLIR System).

II. Results

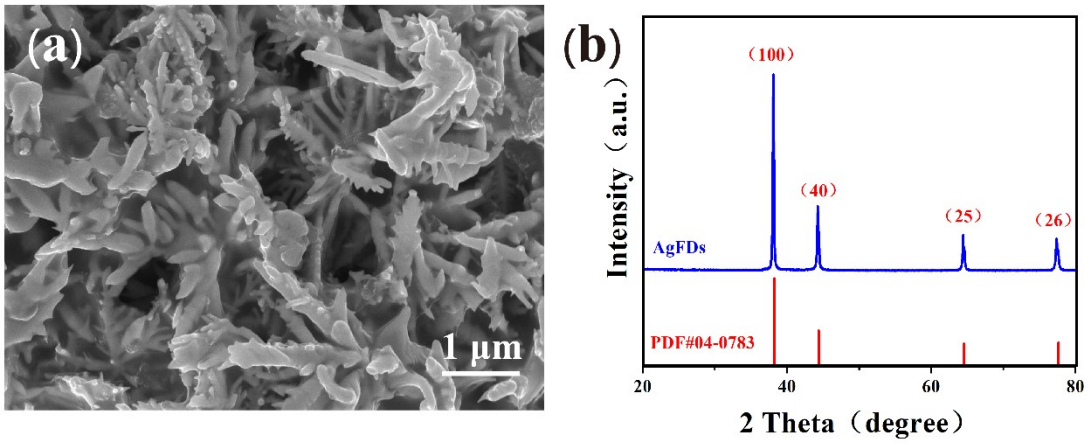

Figure S1 The SEM image (a) and XRD pattern (b) of printed layer of Ag FDs-based conductive ink.

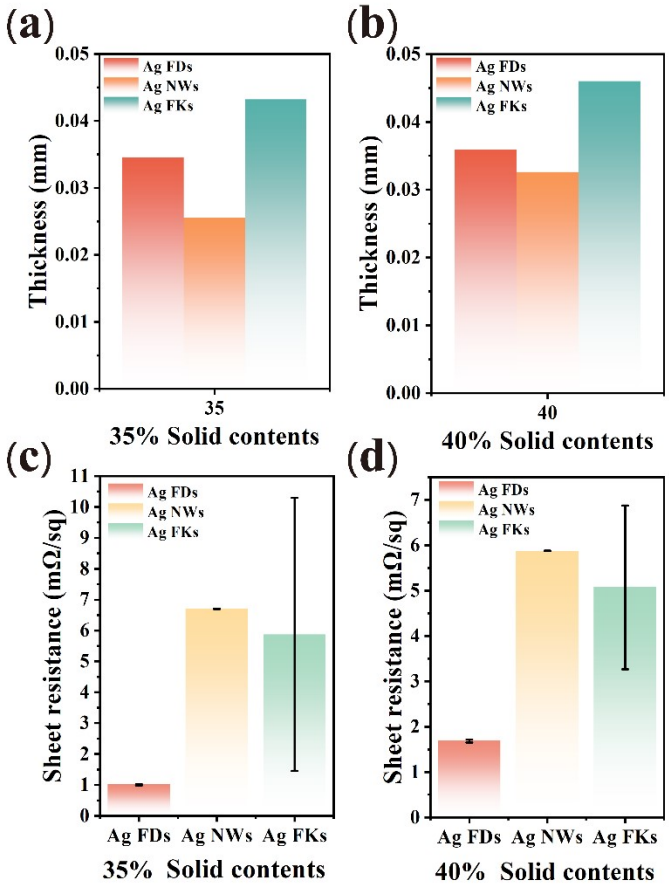

Figure S2 Ink thickness of different Ag nanomaterials (Ag FDs, Ag NWs and Ag FKs)-based inks on paper substrate (a) and PET substrate (b) after printing 3 times. Sheet resistance of Ag nanomaterials (Ag FDs, Ag NWs and Ag FKs)-based inks on paper substrate (c) and PET substrate (d).

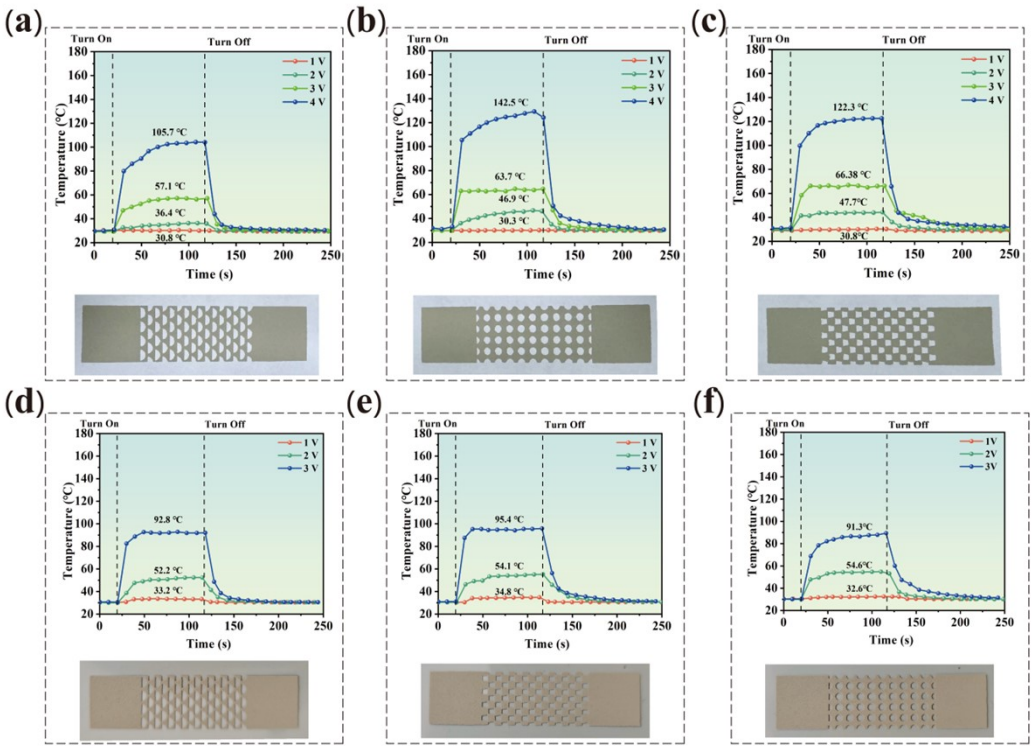

Figure S3 Heating performances of Paper-based (a-c) and PET-based PFHs (d-f) prepared when the printed patterns are semicircular, circular, and square shape.

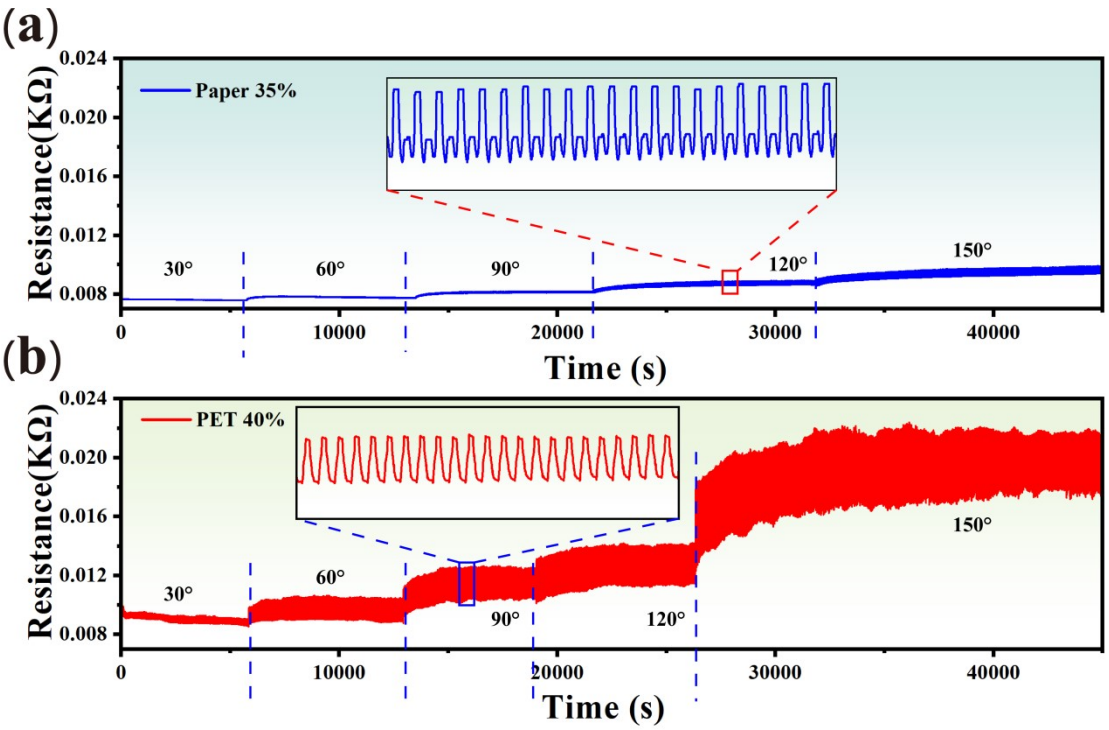

Figure S4 (a) Electrical properties of paper-based FPHs (a) and PET-based FPHs (b) during 500 consecutive bending tests at different angles of 30°, 60°, 90°, 120° and 150°.

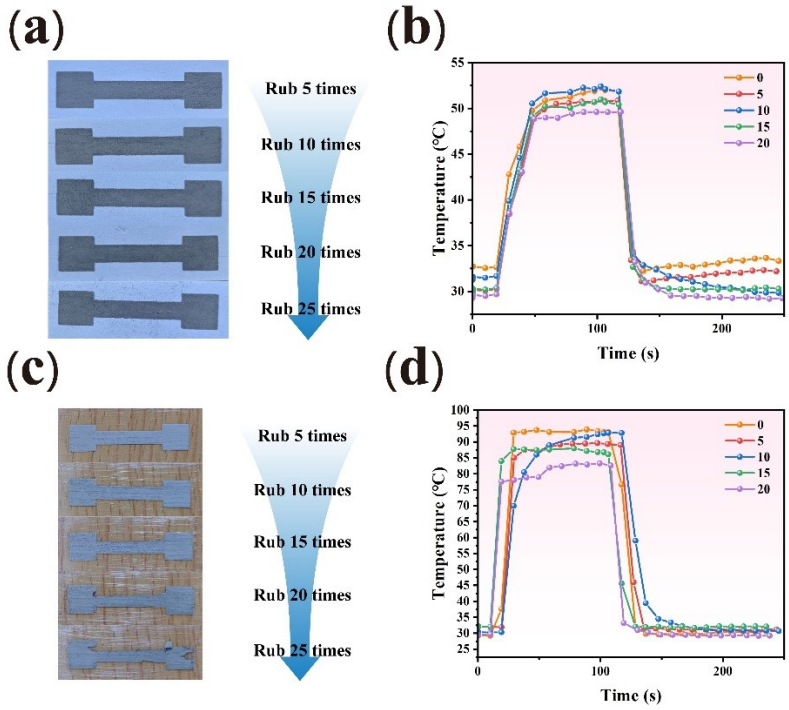

Figure S5 Photos (a) and temperature response curves (b) of the sample printed on the paper substrate being sanded for different times (5, 10, 15, 20 and 25 times) using sandpaper; and photos (c) and temperature response curves (d) of the sample printed on the PET substrate being sanded for different times (5, 10, 15, 20 and 25 times) using sandpaper.

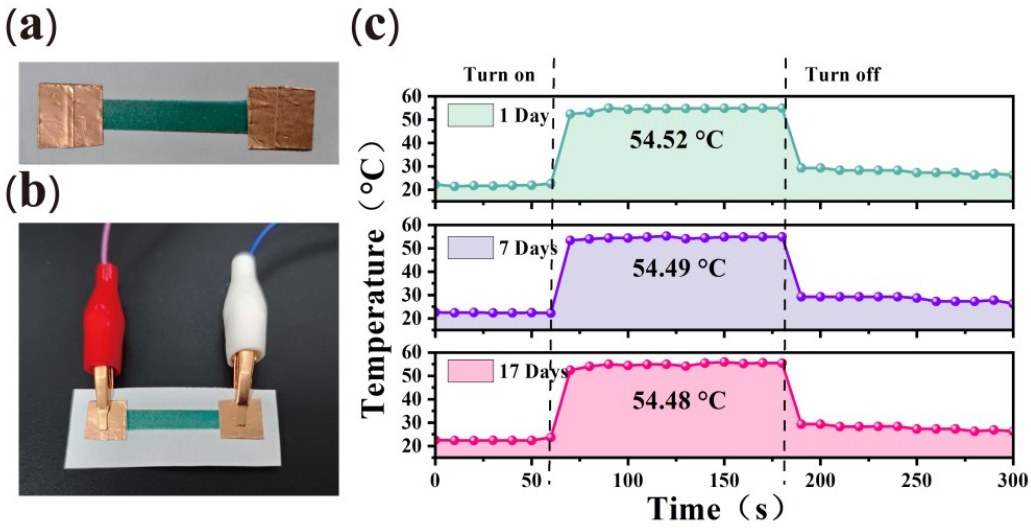

Fig. S6 The long-term heating stability and heating performance of the paper-based

PFH after packaging when the applied voltage is 3 V.

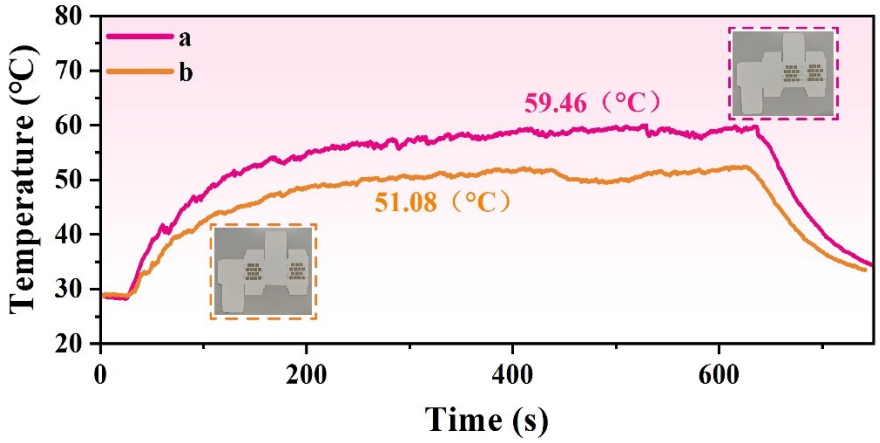

Figure S7 Temperature response curve of heating units that printed on adjacent (a) and non-adjacent sides (b).

Table S1 The comparison of the heating performance of our PHF with the previous literatures.

Used materials	**Heating times (s)**	**Saturation temperature (◦C)**	**Applied voltage (v)**	**References**
CNTs	/	100	20	[1]
CNTs/TPU	/	140	10	[2]
Ag NWs/PUD	300	141	5	[3]
MWCNTs/CB	300	60	24	[4]
Ag NTRs	50	100	7	[5]
Graphene	180	55	80	[6]
GO/graphene nanosheets	60	127.5	40	[7]
Ag NW–PMMA	30	97	5	[8]

Graphene oxide (GO)	360	160	60	[9]
Carbon black	300	200	20	[10]
Ag FDs-based inks	10	123.5	4	This work

References

1. S.-H. Jang, D. Kim and Y.-L. Park. Accelerated Curing and Enhanced Material Properties of Conductive Polymer Nanocomposites by Joule Heating. *Materials* 11 (**2018**) 1775.

2. J. Luo, H. Lu, Q. Zhang, Y. Yao, M. Chen and Q. Li. Flexible carbon nanotube/polyurethane electrothermal films. *Carbon* 110 (**2016**) 343-349.

3. X. Chen, B. Liu, J. Jin, S. Li, S. Li, B. Liao, Z. Sheng and H. Wu. Ultra-flexible and transparent AgNWs-based electrodes for Joule heating. *Materials Science in Semiconductor Processing* 174 (**2024**) 108237.

4. Y. Xia, X. Yu, C. Sheng, C. Liang, H. Huang, Y. Gan, J. Zhang, X. Tao, Z. Xiao and W. Zhang. N991/MWCNTs/PEO composite films with nano SiO2 particles as filler for advanced flexible electric heating elements. *Materials Research Bulletin* 90 (**2017**) 273-279.

5. P. Li, J. G. Ma, H. Y. Xu, D. Lin, X. D. Xue, X. Z. Yan, P. Xia and Y. C. Liu. Flexible transparent heaters based on silver nanotrough meshes. *Journal of Alloys and Compounds* 664 (**2016**) 764-769.

6. L. Cui, K. Cui, H. Ci, K. Zheng, H. Xie, X. Gao, Y. Zhang and Z. Liu. Transparent Electrothermal Heaters Based on Vertically-Oriented Graphene Glass Hybrid Materials. *Nanomaterials* 9 (**2019**) 558.

7. H. Sun, D. Chen, C. Ye, X. Li, D. Dai, Q. Yuan, K. W. A. Chee, P. Zhao, N. Jiang and C.-T. Lin. Large-area self-assembled reduced graphene oxide/electrochemically exfoliated graphene hybrid films for transparent electrothermal heaters. *Applied Surface Science* 435 (**2018**) 809-814.

8. X. He, A. l. Liu, X. Hu, M. Song, F. Duan, Q. Lan, J. Xiao, J. Liu, M. Zhang, Y. Chen and Q. Zeng. Temperature-controlled transparent-film heater based on silver nanowire–PMMA composite film. *Nanotechnology* 27 (**2016**) 475709.

9. S.-Y. Kim, H.-E. Gang, G.-T. Park, H.-B. Jeon and Y. G. Jeong. Microstructure and electrothermal characterization of transparent reduced graphene oxide thin films manufactured by spin-coating and thermal reduction. *Results in Physics* 24 (**2021**) 104107.

10. Z. Xiao, R. Guo, X. He, Y. Gan, J. Zhang, H. Huang, W. Zhang, B. Wang, Y. Han and Y. Xia. Polybenzimidazole/Conductive Carbon Black Composite Driven at Low Voltage for High-Temperature Heaters. *Journal of Electronic Materials* 51 (**2022**) 2652-2662.